

# Magnetic and EPR studies of the $\text{EuFe}_3(\text{BO}_3)_4$ single crystal

V.P. Dyakonov<sup>1,2</sup>, R. Szymczak<sup>1</sup>, A.D. Prokhorov<sup>2</sup>, E. Zubov<sup>2,a</sup>, A.A. Prokhorov<sup>2</sup>, G. Petrakovskii<sup>3</sup>, L. Bezmaternikh<sup>3</sup>, M. Berkowski<sup>1</sup>, V. Varyukhin<sup>2</sup>, and H. Szymczak<sup>1</sup>

<sup>1</sup> Institute of Physics, PAS, 02-668 Warsaw, Al. Lotnikow 32/46, Poland

<sup>2</sup> A.A. Galkin Donetsk Physico-Technical Institute, NANU, 83114 Donetsk, R. Luxembourg str. 72, Ukraine

<sup>3</sup> L.V. Kirenski Institute of Physics, SB of RAS, 660036 Krasnoyarsk, Russia

Received 20 January 2010 / Received in final form 1st June 2010

Published online 17 November 2010 – © EDP Sciences, Società Italiana di Fisica, Springer-Verlag 2010

**Abstract.** Magnetic and electron paramagnetic resonance (EPR) properties of  $\text{EuFe}_3(\text{BO}_3)_4$  single crystals have been studied over the temperature range of 300–4.2 K and in a magnetic field up to 5 T. The temperature, field and orientation dependences of susceptibility, magnetization and EPR spectra are presented. An antiferromagnetic ordering of the Fe subsystem occurs at about 37 K. The easy direction of magnetization perpendicular to the  $c$  axis is determined by magnetic measurements. Below 10 K, we observe an increase of susceptibility connected with the polarization of the Eu sublattice by an effective exchange field of the ordered Fe magnetic subsystem. In a magnetic field perpendicular to the  $c$  axis, we have observed an increase of magnetization at  $T < 10$  K in the applied magnetic field, which can be attributed to the appearance of the magnetic moment induced by the magnetic field applied in the basal plane. According to EPR measurements, the distance between the maximum and minimum of derivative of absorption line of the Lorentz type is equal to 319 Gs. The anisotropy of  $g$ -factor and linewidth is due to the influence of crystalline field of trigonal symmetry. The peculiarities of temperature dependence of both intensity and linewidth are caused by the influence of excited states of europium ion ( $\text{Eu}^{3+}$ ). It is supposed that the difference between the  $g$ -factors from EPR and the magnetic measurements is caused by exchange interaction between rare earth and Fe subsystems via anomalous Zeeman effect.

## 1 Introduction

The general formula of borate crystals with the structure of huntite is  $\text{RE}M_3(\text{BO}_3)_4$ , where RE designates a rare-earth ion and M is a trivalent Fe, Al, Cr or Ga ions [1,2]. Among them, magnetic properties of the rare-earth iron borates  $\text{REFe}_3(\text{BO}_3)_4$  have attracted considerable attention caused by competing magnetic sublattice and magnetoelectric interactions, as well as the manifestation by some iron borates of multiferroic features, which presume the coexistence of magnetic and ferroelectric order parameters [3–11]. These borate crystals show a series of phase transitions, namely, an antiferromagnetic ordering near 40 K as well as a structural phase transition at higher temperatures and a spin reorientation (spin flop) phase transition induced by magnetic field at low temperatures ( $<10$  K) in such ferroborates as  $\text{GdFe}_3(\text{BO}_3)_4$  [4,7,12,13],  $\text{TbFe}_3(\text{BO}_3)_4$  [14],  $\text{DyFe}_3(\text{BO}_3)_4$  [15], (Y, ER)  $\text{Fe}_3(\text{BO}_3)_4$  [16] and  $\text{NdFe}_3(\text{BO}_3)_4$  [17]. A structural phase transitions at higher temperatures were also observed for compounds with Tb [14] and RE = Eu–Ho [18].

According to the results of magnetization, specific heat, and neutron diffraction measurements, the

peculiarities of a magnetic ordered state of RE-ferroborates are caused by the properties of the lanthanide and the transition metals subsystems and their interactions. It determines also the orientation of the magnetic moments of iron with respect to the crystallographic axes.

Despite number of publications on properties of RE-ferroborates, some aspects of their low temperature magnetic behavior need to be clarified.

Until now, only one paper [3] has studied the changes of magnetic susceptibility and specific heat of the europium iron borate  $\text{EuFe}_3(\text{BO}_3)_4$  in an arbitrary direction. According to the specific heat data, the ordering temperature of  $\text{EuFe}_3(\text{BO}_3)_4$  is equal to  $T_N = 34$  K. At the same time, a susceptibility anomaly related to AFM transition takes place at temperature of  $T_N = 40$  K. In addition to the AFM transition at 34 K, another anomaly has been found in the specific heat vs. temperature curve at 88 K which is related to the structural phase transition.

The majority of known papers in which rare-earth ferroborates crystals were investigated were devoted to study the properties of these materials in a magnetically ordered state. Electron paramagnetic resonance (EPR), being a powerful tool to obtain valuable information regarding both the paramagnetic state and interplay of different interactions in ferroborates, was not used for these purposes.

<sup>a</sup> e-mail: zubov@fti.dn.ua

This technique is based on a study of the temperature and orientation dependences of various EPR parameters, such as the resonance field,  $g$ -factor, shape and width of absorption lines and resonance intensity.

In this paper, our attention has been focused on magnetic and resonance properties of  $\text{EuFe}_3(\text{BO}_3)_4$ . The problem is complicated because two different kinds of magnetic ions ( $\text{Eu}^{3+}$  and  $\text{Fe}^{3+}$ ) exist in this material. Therefore, it is interesting to understand both the magnetic ordering of the iron and europium subsystems, as well as the properties of the paramagnetic phase. The magnetic properties and the EPR spectra in  $\text{EuFe}_3(\text{BO}_3)_4$  single crystal were first investigated over a wide temperature and magnetic field range along the different crystallographic axes. Through these measurements, the peculiarities of magnetic and resonance properties of  $\text{EuFe}_3(\text{BO}_3)_4$  were elucidated. We have established the additional contribution of  $\text{Eu}^{3+}$  ions to inter-sublattice anisotropy.

## 2 Sample preparation and experimental

The single crystal of  $\text{EuFe}_3(\text{BO}_3)_4$  used for measurements was grown from a solution in a melt, as described in reference [19], at the Institute of Physics (Krasnoyarsk).

The space group, lattice constants and orientation of the axes in the crystal were obtained at room temperature with four-circle kappa-geometry diffractometer KM4 (by Kuma-Diffractometer) using monochromatized  $\text{CuK}\alpha$  radiation. The structure of  $\text{EuFe}_3(\text{BO}_3)_4$  determined belongs to the space group R32. The lattice parameters are  $a = 9.554 \text{ \AA}$ ,  $c = 7.576 \text{ \AA}$ , and  $V = 598.9 \text{ \AA}^3$ . The measurements have been carried out on the oriented  $\text{EuFe}_3(\text{BO}_3)_4$  single crystal the size of  $3 \times 2 \times 1.5 \text{ mm}^3$ .

The temperature and field dependences of magnetization of  $\text{EuFe}_3(\text{BO}_3)_4$  have been measured by a SQUID over the temperature range of 4.2–300 K and in an applied magnetic field up to 5 T. Magnetic field was applied along the  $a$  and  $c$  axes.

The measurements of EPR spectra have been performed with a X-band Bruker spectrometer with high-frequency modulation in a temperature interval from 4.2 to 300 K. A flowing helium-gas cryostat was used to alter the temperature of the sample.

## 3 Results of magnetization studies

The behavior of susceptibility ( $M/H$ ) as a function of temperature in an applied magnetic field of 6 kOe parallel and perpendicular to the hexagonal  $c$  direction is seen in Figure 1. The  $M/H(T)$  dependence in field of 4 kOe parallel to the  $a$  and  $b$  axes (inset of Fig. 1) shows that an anisotropy in the  $a$ - $b$  plane is absent or is very small. As seen in Figure 1, the  $M/H(T)$  dependence has a maximum at approximately of 37 K, which is characteristic of the onset of antiferromagnetic (AFM) ordering of the Fe subsystem. Below  $T_{min} = 15 \text{ K}$ , the increase of susceptibility is evidently connected with the magnetic polarization of the Eu sublattice by an effective exchange field

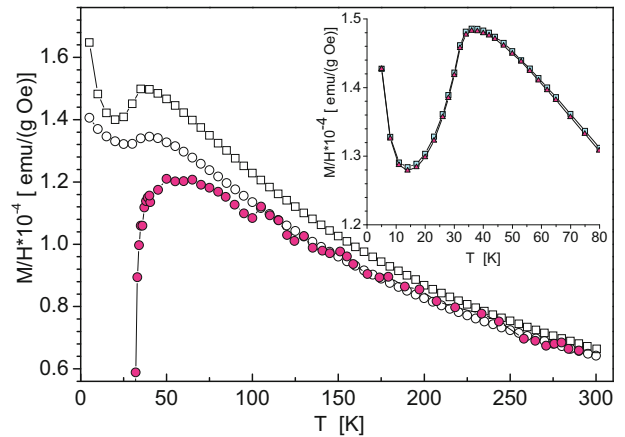


**Fig. 1.** (Color online) Temperature dependences of susceptibility ( $M/H$ ) parallel (open circles) and perpendicular (squares) to the  $c$  axis in a magnetic field of 6 kOe. Temperature dependence of normalized integral intensity of EPR line (filled circles) at the orientation of the magnetic field along the  $c$  crystal axes. Inset: temperature dependences of susceptibility parallel to the  $a$  (squares) and  $b$  (triangles) axes in a magnetic field of 4 kOe.

of the ordered Fe magnetic subsystem. However, the low temperature peak resulted from a spin reorientation (spin-flop) phase transition, as in the case of ferrobates with the  $\text{Gd}^{3+}$ ,  $\text{Dy}^{3+}$  and  $\text{Nd}^{3+}$  ions [7,15,17], is not observed up to 4.2 K. Figure 1 clearly illustrates that at low temperatures, the easy direction of magnetization is oriented perpendicular to the hexagonal  $c$  axis. An insignificant difference between the ZFC and FC magnetization has been found.

The temperature dependence of susceptibility and change of integral intensity of EPR line with temperature are known to be proportional to each other. The normalized integral intensity presented in Figure 1 was obtained by using the ratio of integral intensity to susceptibility along the  $c$  axis at 6 kOe at 300 K. Figure 1 shows that at high temperatures, the temperature contribution of  $\text{Eu}^{3+}$  ions may be neglected. The susceptibility is seen to become larger than the integral intensity related to  $\text{Fe}^{3+}$  subsystem with decreasing temperature. The low temperature behavior of susceptibility really reflects the substantial influence of the  $\text{Eu}^{3+}$  ions.

The temperature dependence of  $M/H$  does not exhibit the anomaly at high temperature observed in the specific heat vs. temperature curve and connected with structural transition [3,14]. The temperature dependences of the reciprocal susceptibility show a linear behavior above the magnetic transition temperature up to 300 K and follow the Curie-Weiss law (Fig. 2).

To definite the microscopic parameters of interaction we have carried out fitting of the experimental data to the Curie-Weiss (CW) law

$$\chi_i = \frac{C_i}{T - \theta_i}, \quad (1)$$

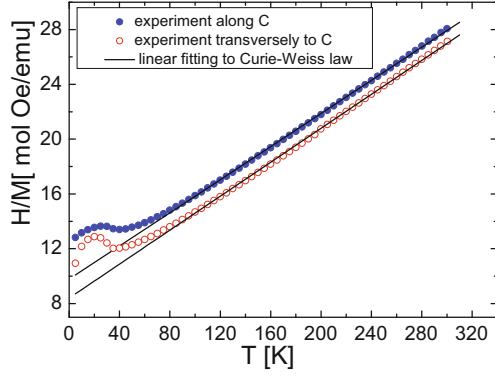


**Fig. 2.** (Color online) Temperature dependences of reciprocal susceptibility parallel (filled circles) and perpendicular (open circles) to the  $c$  axis in a magnetic field of 6 kOe.

where  $\theta$  is the paramagnetic CW temperature, the Curie constant  $C_i = \frac{1}{3k_B} S(S+1) \mu_B^2 g_i^2 N_A$ ,  $S = 5/2$  is the Fe ion spin,  $\mu_B$  the Bohr magneton,  $g_i$  the  $g$ -factor along the  $i$  axis,  $N_A$  the Avogadro constant.

The effective magnetic moment,  $\mu_{eff}$ , can be determined as the sum of the contributions of the  $\text{R}^{3+} = \text{Eu}^{3+}$  and  $\text{Fe}^{3+}$  ions [20–22]:

$$\mu_{eff}^2 = \mu_{eff}^2(\text{R}^{3+}) + 3\mu_{eff}^2(\text{Fe}^{3+}), \quad (2)$$

where

$$\begin{aligned} \mu_{eff}^2(\text{R}^{3+}) &= g_{\text{R}^{3+}}^2 J(J+1) \mu_B^2 \\ \mu_{eff}^2(\text{Fe}^{3+}) &= g_{\text{Fe}^{3+}}^2 S(S+1) \mu_B^2. \end{aligned}$$

Since the  $\text{Eu}^{3+}$  ion with an  $4f^6$  electronic configuration of the  ${}^7\text{F}_0$  ground state has the angular momentum  $J = 0$  ( $J = S - L = 0$ , where  $L$  and  $S$  are the orbital and the spin moments, respectively), the magnetic moment  $\mu_{eff}$  for  $\text{EuFe}_3(\text{BO}_3)_4$  is determined mainly by the  $\text{Fe}^{3+}$  subsystem. Taking into account that  $g_{\text{Fe}^{3+}}^2 = 2$  and the spin  $S = 5/2$  for high-spin state of  $\text{Fe}^{3+}$  ions, the calculated  $\mu_{eff}$  value is equal to  $10.25 \mu_B$ .

The paramagnetic CW temperatures,  $\theta$  and  $\theta$ , for a magnetic field  $H = 6$  kOe applied in geometry  $H \parallel c$  and  $H \perp c$  are equal to  $-162$  and  $-136$  K, respectively. It should be noted that the obtained values are high enough in comparison with  $T_N = 37$  K. The negative Curie-Weiss temperatures confirm that the magnetic exchange interactions in the studied compound are antiferromagnetic.

Substituting the experimental value of  $\theta$  in the (A.4) expression (Appendix A), and the phase transition temperature equal to  $1.5T_N$  in the (A.5) expression calculated with taking into account of fluctuations, we obtain the following relations :

$$\begin{aligned} J_{12}(0) + B_{12} &= -18.6 \text{ K} \\ J_{11}(0) &= -9.1 \text{ K}. \end{aligned}$$

The obtained values indicate the large total value of inter-sublattice exchange interaction and anisotropy as compared with intra-sublattice exchange.

The paramagnetic temperature,  $\theta$ , perpendicular to the  $c$  axis can be determined as

$$\theta = \frac{2}{3} S(S+1) (J_{12}(0) + J_{11}(0)). \quad (3)$$

This relation follows from the (A.3) expression at  $\tilde{H}_i = 0$  and  $\tilde{h}_i \neq 0$ ,  $\langle S_1^x \rangle = \langle S_2^x \rangle = \langle S^x \rangle$ .

Subtracting (3) from the (A.4) expression we have

$$\theta - \theta = \frac{2}{3} S(S+1) B_{12}, \quad (4)$$

where  $\theta - \theta = -26$  K, that gives the anisotropy constant  $B_{12} = -4.5$  K and the total value of isotropic exchange  $J_{12}(0) + J_{11}(0) = -23.2$  K. As a result, the AFM inter- and intra- sublattice exchange parameters are equal to  $J_{12}(0) = -14.1$  and  $J_{11}(0) = -9.1$  K, respectively.

The obtained data point out a large easy plane anisotropy. Therefore, to realize a spin reorientation phase transition in  $\text{EuFe}_3(\text{BO}_3)_4$  (as in  $\text{GdFe}_3(\text{BO}_3)_4$  [4,7]), the exchange field of saturation,  $H_E$ , for a model with anisotropy exchange interactions should be equal to

$$H_E = 2S \{2|J_{12}(0)| - B_{12}\} = 163 \text{ K},$$

where the constant  $B_{12}$  of inter-sublattice exchange anisotropy is determined in Appendix A.

Then the field of spin-flop transition,  $H_{sf}$ , will be equal to

$$H_{sf} = \sqrt{-2SB_{12}H_E} = 60.3 \text{ K}.$$

The  $g$ -factor values are obtained to be equal to 2.24 and 2.22 for the parallel and perpendicular directions to the  $c$  axis, respectively. Then, the effective magnetic moments parallel and perpendicular to the  $c$  axis obtained from the CW law will be equal to  $11.5$  and  $11.4 \mu_B$ , respectively. The difference between the above obtained values of  $\mu_{eff}$  and the calculated value of  $10.25 \mu_B$  is evidently connected with the contribution of the  $\text{Eu}^{3+}$  subsystem.

An interaction between  $\text{Eu}^{3+}$  and  $\text{Fe}^{3+}$  sublattice in  $\text{EuFe}_3(\text{BO}_3)_4$  causes the anisotropy of the exchange interactions of the  $\text{Fe}^{3+}$  ions. Since the angular momentum of  $\text{Eu}^{3+}$  is zero, the bond between Eu and  $\text{Fe}^{3+}$  ions is realized via second-order Zeeman effect [21] (Appendix B).

From the (B.11) expression (Appendix B) at  $\Delta_1 = 480$  K [21] and  $\Delta g_z = 0.24$  we obtain the value of exchange interaction between RE and  $\text{Fe}^{3+}$  ions along the  $c$  axis equal to  $J_z = 4.8$  K. Using the  $J_z$  value and the relation (B.8) the value of exchange interaction between RE and  $\text{Fe}^{3+}$  ions in the  $ab$  plane is obtained to be equal to  $J_x = 17.1$  K.

Additional information on the magnetic properties was obtained by the measurements of both the susceptibility in the applied magnetic field and  $M(H)$  isotherms. As seen in Figure 3, the paramagnet-antiferromagnet phase transition temperature in the magnetic field does not change. However, the susceptibility is highly dependent on the applied magnetic field at  $T < T_N$ . Both the susceptibility and  $T_{min}$  increase as the magnetic field changes from 0.1 to 1.2 kOe.

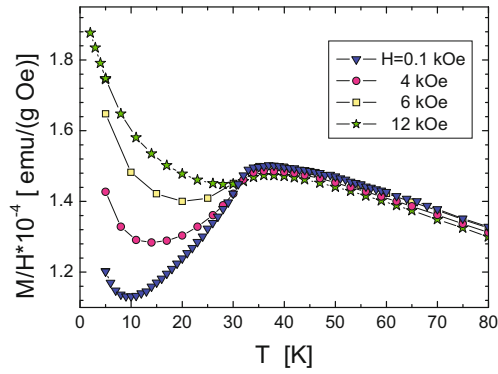


**Fig. 3.** (Color online) Susceptibility vs. temperature in the applied magnetic field perpendicular to the  $c$  axis.

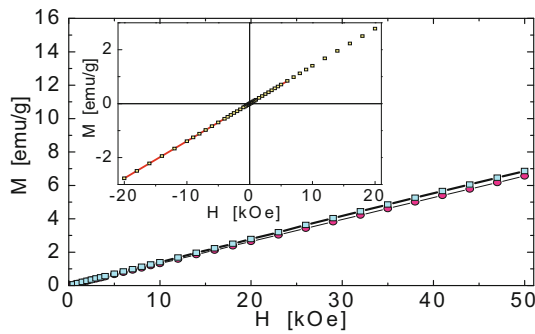


**Fig. 4.** (Color online) Field dependences of magnetization parallel to the  $c$  axis at 5 (squares) and 25 (filled circles) K. Inset to Figure 4 –  $M(H)$  hysteresis curves in the magnetic field changed from +20 kOe to –20 kOe.

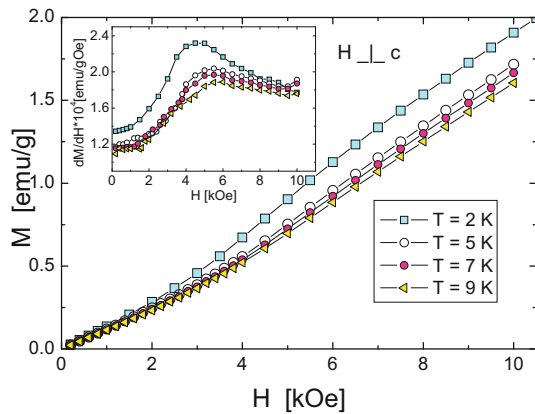


**Fig. 5.** (Color online) Field dependences of magnetization perpendicular to the  $c$  axis at different temperatures. Inset : the derivatives magnetization  $dM/dH$  vs.  $H$ .

The field dependences of magnetization parallel and perpendicular to the  $c$  axis are plotted in Figures 4 and 5, respectively. At low temperatures, the  $M(H)$  dependences are different for  $H \parallel c$  and  $H \perp c$ . When the magnetic field is parallel to the  $c$  axis (Fig. 4), the  $M(H)$  dependences at 5 and 25 K are linear in the range of  $0 < H < 50$  kOe, i.e. the applied magnetic field does not influence the iron spin direction and magnetization vanishes at zero field. This behavior indicates that the ground state of  $\text{EuFe}_3(\text{BO}_3)_4$  is a compensated AFM. The  $M(H)$

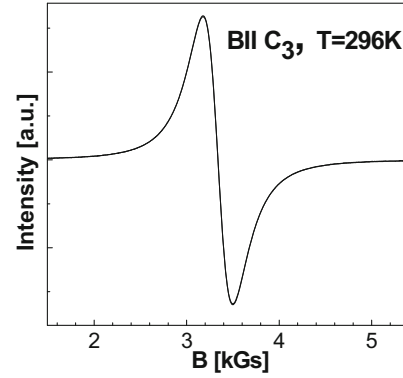


**Fig. 6.** Experimental EPR curve for the orientation  $B \parallel C_3$  at  $T = 296$  K.

hysteresis curve measurements in magnetic field changed from +20 kOe to –20 kOe show that the coercive field and remanence are equal to zero (Inset to Fig. 4).

In a field perpendicular to the  $c$  axis, the  $M(H)$  dependence at 25 K is also linear in the range of  $0 < H < 50$  kOe. However, at  $T < 10$  K, an anomaly in the  $M(H)$  isotherms was observed (see an inset in Fig. 5). This can be attributed to the occurrence of the magnetic moment in the basal plane induced by the magnetic field. It is seen that the value of field, at which an anomaly occurs, decreases with decreasing temperature.

## 4 Results of EPR studies

The EPR spectra and their parameters in  $\text{EuFe}_3(\text{BO}_3)_4$  single crystal were first studied over a wide temperature range along the different crystallographic axes. The experimental EPR curve for the orientation  $\mathbf{B} \parallel C_3$  at  $T = 296$  K is shown in Figure 6.

We observe a paramagnetic resonance line, which owes its origins to trivalent iron ( $\text{Fe}^{3+}$ ) ions (an electronic configuration of  $3d^5$ , spin  $S = 5/2$ , the orbital moment is equal to zero). Despite of splitting of the ground state of  $\text{Fe}^{3+}$  ion in crystal field, the characteristic fine structure in the EPR spectrum is absent. It is connected with a so-called exchange narrowing which manifests itself when the exchange interaction value becomes larger than the interval between lines of fine structure, and an averaging of anisotropic interactions takes place. As a result there is a single symmetric Lorentzian line. The criterion of exchange narrowing of resonance line is the ratio  $\langle \Delta\nu \rangle_{1/2} \approx \langle \Delta\nu^2 \rangle / (J/h)$  [23], where  $\langle \Delta\nu \rangle_{1/2}$  is the absorption widthline, the second moment  $\langle \Delta\nu^2 \rangle$  is due to interactions (magnetic dipole-dipole, hyperfine and interaction with a crystal field) causing splitting of lines and  $J/h$  the exchange energy.

The  $g$ -factors were calculated using the angular dependence of EPR line (Fig. 7) and standard formula:

$$g^2 = g^2 \cos^2 \vartheta + g^2 \sin^2 \vartheta, \quad (5)$$

where  $g \pm 2.010 \pm 0.001$ ;  $g \pm 2.015 \pm 0.001$  are the values of the  $g$ -factors parallel and perpendicular to the  $c$



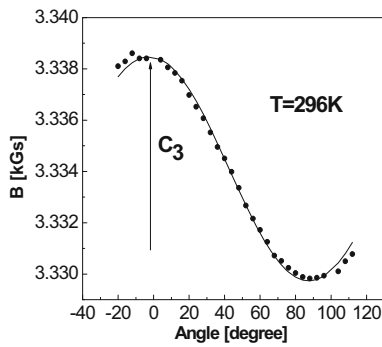


**Fig. 7.** Experimental angular dependence at  $T = 296$  K EPR (points) in the  $a$ - $c$  plane at  $T = 296$  K. The line was obtained using the equation  $B = h\nu/g\mu_B$ .

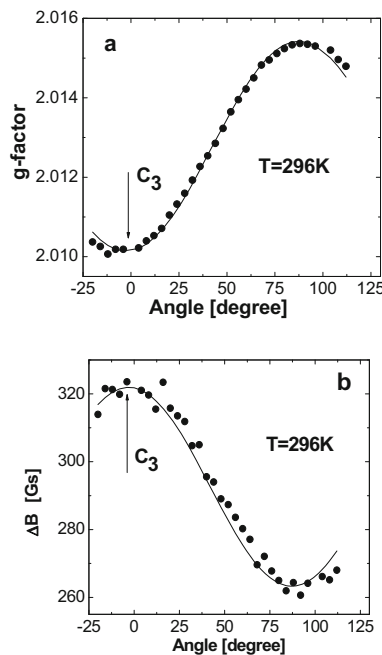


**Fig. 8.** The experimental (points) and calculated (line) angular dependences of  $g$ -factor (a) and linewidth (b) observed in the  $a$ - $c$  plane at  $T = 296$  K.

axis,  $\vartheta$  the angle showing the deviation of magnetic field from the  $c$  axis. The experimental (points) and calculated (line) angular dependences of the  $g$ -factor are shown in Figure 8a. The  $g$ -factor values agree with the data known from EPR investigations of trivalent iron. A difference between EPR and susceptibility data regarding  $g$ -factors is connected with an interaction between  $\text{Eu}^{3+}$  and  $\text{Fe}^{3+}$  ions and really reflects the substantial influence of the  $\text{Eu}^{3+}$  ions. Indeed, the observed EPR line owes its origin to trivalent iron ( $\text{Fe}^{3+}$ ) ions. The interaction between  $\text{Fe}^{3+}$  and  $\text{Eu}^{3+}$  subsystems is a collective effect that is fixed by susceptibility measurement. Since the energy interval between the ground state and first excited state of  $\text{Eu}^{3+}$  ion is on the order of  $300 \text{ cm}^{-1}$  and the temperature interval of fitting of susceptibility to the Curie-Weiss law is from 100 to 300 K, we have the mixture of the singlet and excited levels of the  $\text{Eu}^{3+}$  ions with nonzero magnetic quantum numbers. In reference [21], it was pointed

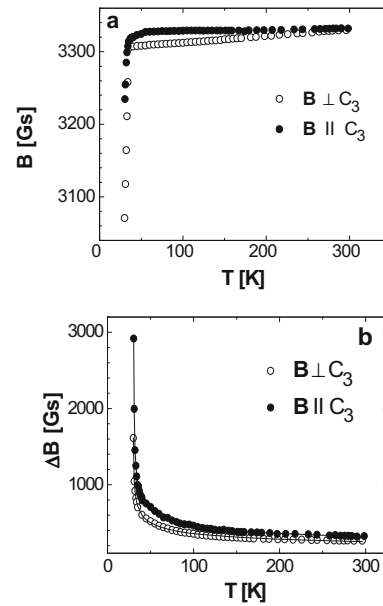


**Fig. 9.** Experimental (points) temperature dependences of resonance field (a) and absorption linewidth (b). Calculated temperature dependence of absorption linewidth using the function of  $\Delta B = A + B/(T - T_N)^k$  is presented by line in Figure 9b.

out that although the ground state of  $\text{Eu}^{3+}$  ion is the state with  $J = 0$ , it is paramagnet with the magnetic moment caused by an influence the excited levels (the second-order Zeeman effect).

An anisotropy of both  $g$ -factor and linewidth was observed when the magnetic field is rotated from the  $c$  axis to the perpendicular plane. In the plane perpendicular to the  $c$  axis, an anisotropy is not observed. These EPR data correlate with the behavior of susceptibility along the corresponding crystallographic axes (the inset of Fig. 1).

Experimental (points) and fitted (line) angle dependences of linewidth (at  $T = 296$  K) shown in Figure 8b are caused by an anisotropic influence of a crystal field. The distance between the maximum and minimum of derivative of absorption line is equal to 319 Gs. The EPR spectrum in the magnetic field parallel to the  $c$  axis has a larger linewidth (the distance between the extreme lines of the spectrum) than in perpendicular orientation. This difference is proportional to the value of  $A(3 \cos^2 \vartheta - 1)$ , where the value characterizes the interaction responsible for the anisotropy and the order of magnitude of the linewidth. The  $A$  correction factor is proportional to the value of splitting of the ground state of  $\text{Fe}^{3+}$  ion which in spin Hamiltonian is described by the  $D(b_2^0)$  parameter.

Figure 9a shows the temperature dependences of resonance field,  $B(T)$ , when the magnetic field is oriented parallel to the  $c$  axis and for field  $H \perp c$ . Both dependences are similar. The resonant field value does not change when the room temperature decreases to the phase transition temperature. At AFM phase transition, the resonant field value sharply decreases, while the absorption line broadens and is practically not observed below 30 K (Fig. 9b). The behavior of absorption linewidth above the phase transition temperature  $T_N$  is caused by the fact that

fluctuations begin to play a significant role. The critical phenomena arise and the parameters of system can be described by means of a power series of the parameter  $\alpha = (T - T_N)/T_N$ . Near the phase transition temperature, the thermodynamic behavior will be defined by the main member of series of expansion. Experimental temperature dependences of linewidth (Fig. 9b) are described precisely enough by the function of  $\Delta B = A + B/(T - T_N)^k$ , where for the orientation  $B \parallel C_3$   $T_N = 30.3$  K,  $A = 107.9$ ,  $B = 1655.2$  and  $k = 0.37$  and for the orientation  $B \perp C_3$   $T_N = 29.7$  K,  $A = 17.6$ ,  $B = 1123.6$  and  $k = 0.28$ .

The temperature dependence of integral intensity obtained by double integration of the derivative of absorption line is one more feature of the EPR spectrum. When temperature decreases, the integral intensity increases twice and then decreases. Such behavior of the EPR intensity close to  $T_N$  can be caused by the development of short-range AFM correlations, which do not give the contribution to intensity of the absorption line.

## 5 Conclusion

In summary, the susceptibility, magnetization and EPR data provide useful information on low temperature magnetic properties of this novel family of complex metaloxide compounds. Both AFM ordering of the Fe subsystem at about 37 K and the easy direction of magnetization perpendicular to the  $c$  axis were established. The increase of susceptibility below 15 K is connected with the magnetic polarization of the Eu sublattice by the ordered Fe magnetic subsystem. The low temperature anomaly in the  $M(H)$  isotherm in field perpendicular to the  $c$  axis is connected to the occurrence of the magnetic moment in the basal plane induced by magnetic field. The single EPR line observed is shown to be the result of exchange interaction between ions of trivalent iron, which averages an influence of crystalline field and magnetic dipole-dipole interactions. The temperature dependence of both linewidth and its integral intensity depends on the considerable degree on interaction of iron ions with excited states of trivalent europium. The anisotropy of both  $g$ -factor and linewidth is due to the influence of crystalline field of trigonal symmetry. The difference between  $g$ -factor values obtained from EPR and magnetic measurements is supposed to be caused by exchange interaction between rare earth and Fe subsystems via anomalous Zeeman effect. The peculiarities of temperature dependence of linewidth above the  $T_N$  temperature are caused by the fact that fluctuations begin to play a significant role and critical phenomena arise.

A.A. Prokhorov is grateful to Mianowski Fund for financial support.

## Appendix A

In the general case of the antiferromagnetic model with two sublattices and a single axis anisotropy (denoted by

$z$ -axis) the Heisenberg Hamiltonian may be presented as

$$\begin{aligned} \hat{H} = & - \sum_{i \neq j} J_{ij} \mathbf{S}_i \mathbf{S}_j - \sum_{\alpha \neq \beta} J_{\alpha\beta} \mathbf{S}_\alpha \mathbf{S}_\beta - \sum_{i\alpha} J_{i\alpha} \mathbf{S}_i \mathbf{S}_\alpha \\ & - \sum_{i \neq j} B_{ij} S_i^z S_j^z - \sum_{\alpha \neq \beta} B_{\alpha\beta} S_\alpha^z S_\beta^z - 2 \sum_{i \neq j} B_{i\alpha} S_i^z S_\alpha^z \\ & - H \left( \sum_i S_i^z + \sum_\alpha S_\alpha^z \right), \end{aligned} \quad (\text{A.1})$$

where Latin and Greek symbols correspond to sites of different magnetic sublattices,  $J_{ij}$ ,  $J_{\alpha\beta}$ , and  $B_{ij}$ ,  $B_{\alpha\beta}$  are intra-sublattice isotropic and anisotropic parts of the pair superexchange interactions, respectively, and  $J_{i\alpha}$  and  $B_{i\alpha}$  correspond to inter-sublattice isotropic and anisotropic parts of the pair superexchange interactions, respectively. For simplicity, the applied magnetic field in (A.1) is aligned along the  $z$  axis and measured in  $\mu_B g$  units. It is easy to obtain the mean field approximation of the Hamiltonian (A.1):

$$\begin{aligned} \hat{H}_{MF} = & -2J_{11}(0) \langle \mathbf{S}_1 \rangle \sum_i \mathbf{S}_i - 2J_{11}(0) \langle \mathbf{S}_2 \rangle \sum_\alpha \mathbf{S}_\alpha \\ & - 2J_{12}(0) \langle \mathbf{S}_1 \rangle \sum_\alpha \mathbf{S}_\alpha - 2J_{12}(0) \langle \mathbf{S}_2 \rangle \sum_i \mathbf{S}_i \\ & - 2B \langle S_1^z \rangle \sum_i S_i^z - 2B \langle S_2^z \rangle \sum_\alpha S_\alpha^z \\ & - 2B_{12} \langle S_1^z \rangle \sum_{i \neq j} S_\alpha^z - 2B_{12} \langle S_2^z \rangle \sum_{i \neq j} S_i^z \\ & - H \left( \sum_i S_i^z + \sum_\alpha S_\alpha^z \right). \end{aligned}$$

Here, the mean spins  $\langle \mathbf{S}_1 \rangle$  and  $\langle \mathbf{S}_2 \rangle$  are denoted as follows:  $\langle \mathbf{S}_1 \rangle = \langle \mathbf{S}_i \rangle = \langle \mathbf{S}_j \rangle$ ,  $\langle \mathbf{S}_2 \rangle = \langle \mathbf{S}_\alpha \rangle = \langle \mathbf{S}_\beta \rangle$  and the parameters of Weiss isotropic exchange fields are denoted as  $J_{11}(0) = \sum_{i(\neq j)} J_{ij} = \sum_{\alpha(\neq\beta)} J_{\alpha\beta}$  and  $J_{12}(0) = \sum_i J_{i\alpha} = \sum_\alpha J_{\alpha j}$  for intra- and inter-sublattice interactions, respectively. Similarly, the contributions connected with anisotropic fields are expressed as  $B = \sum_{i(\neq j)} B_{ij} = \sum_{\alpha(\neq\beta)} B_{\alpha\beta}$  and  $B_{12} = \sum_i B_{i\alpha} = \sum_\alpha B_{\alpha j}$  for intra- and inter-sublattice interactions, respectively.

Neglecting the in-plane anisotropy one can write the free  $F$  energy for two sites belonging to the first and second sublattices, respectively:

$$\begin{aligned} F = & J_{11}(0) \sum_{i=1}^2 (\langle S_i^z \rangle^2 + \langle S_i^x \rangle^2) + 2J_{12}(0) (\langle S_1^z \rangle \langle S_2^z \rangle \\ & + \langle S_1^x \rangle \langle S_2^x \rangle) + B (\langle S_1^z \rangle^2 + \langle S_2^z \rangle^2) + 2B_{12}(0) \\ & \times \langle S_1^z \rangle \langle S_2^z \rangle - T (\ln Z_1 + \ln Z_2). \end{aligned} \quad (\text{A.2})$$

The entropy contributions

$$-T \ln Z_i = -T S p \left( \exp \left( -\hat{H}_{0i}/T \right) \right),$$

for  $i$ th sublattice are determined by the corresponding Hamiltonian  $\hat{H}_{0i}$ :

$$\hat{H}_{0i} = -\tilde{H}_i S_i^z - \tilde{h}_i S_i^x,$$

where the effective Weiss fields  $\tilde{H}_i$  and  $\tilde{h}_i$  along the  $z$  and  $x$  axes of  $i$ th sublattice. At  $i \neq j$  they have the following form

$$\begin{aligned} \tilde{H}_i &= H + 2(J_{11}(0) + B) \langle S_i^z \rangle + 2(J_{12}(0) + B_{12}) \langle S_j^z \rangle \\ \tilde{h}_i &= 2J_{11}(0) \langle S_i^x \rangle + 2J_{12}(0) \langle S_j^x \rangle. \end{aligned} \quad (\text{A.3})$$

The free energy (A.2) describes thermodynamics properties of the ferro- (FM), antiferro- (AFM), paramagnetic (PM) and spin-flop (SF) phases. In PM phase  $\tilde{h}_i = 0$  and sublattice magnetization induced by applied magnetic field  $\langle S_1^z \rangle = \langle S_2^z \rangle = \langle S^z \rangle$ . Then the paramagnetic temperature  $\theta$  of an anisotropic two-sublattices Heisenberg antiferromagnet in the direction parallel to the  $c$  axis is determined as

$$\theta = \frac{2}{3} S(S+1) (J_{12}(0) + B_{12} + J_{11}(0)) + B. \quad (\text{A.4})$$

It will be shown that the anisotropy of inter- and intra-sublattice exchange interactions is a result of exchange interactions of  $\text{Eu}^{3+}$ - $\text{Fe}^{3+}$ . Taking into account that the influence of the next nearest neighbors on isotropic exchange is essentially smaller than the influence of the nearest ones, the anisotropy of intra-sublattice exchange interactions,  $B$ , can be neglected.

In AFM phase we have  $\langle S_1^z \rangle = -\langle S_2^z \rangle = \langle S^z \rangle$ . The Néel temperature in a molecular field approximation is expressed as

$$T_N = \frac{2}{3} S(S+1) (-J_{12}(0) - B_{12} + J_{11}(0)). \quad (\text{A.5})$$

## Appendix B

In accordance with reference [22], the Hamiltonian of the interaction between RE and  $\text{Fe}^{3+}$  ions has the form

$$\hat{H}_{\text{Re}\check{\text{S}}\text{Fe}} = -2J(L, L_z) \mathbf{S}_{\text{Re}} \mathbf{S}_{\text{Fe}}, \quad (\text{B.1})$$

where anisotropic exchange parameter  $J(L, L_z)$  can be expanded in terms of tensor-operators of orbital RE moment determined by the local crystal field symmetry of the surrounding ions. In the simplest case, it can be presented as a tensor  $\hat{\mathbf{A}}$  [22]:

$$\hat{\mathbf{A}} = J_0 \begin{pmatrix} 1 - \frac{9}{2}G_2^0 & 0 & 0 \\ 0 & 1 - \frac{9}{2}G_2^0 & 0 \\ 0 & 0 & 1 + 9G_2^0 \end{pmatrix},$$

where  $J_0$  is the isotropic exchange parameter. Then Hamiltonian (B.1) is written as

$$\hat{H}_{\text{Re}\check{\text{S}}\text{Fe}} = -2\mathbf{S}_{\text{Re}} \hat{\mathbf{A}} \mathbf{S}_{\text{Fe}}. \quad (\text{B.2})$$

Equation (B.2) characterizes the single axis character of the anisotropy with constant  $G_2^0$  and is equitable in the first nonvanishing order of the perturbation theory with Hamiltonian (B.1). In mean field approximation one can write equation (B.2) as

$$\hat{H}_{\text{Re}\check{\text{S}}\text{Fe}}^{MF} = -2\langle \mathbf{S}_{\text{Re}} \rangle \hat{\mathbf{A}} \mathbf{S}_{\text{Fe}} - 2\mathbf{S}_{\text{Re}} \hat{\mathbf{A}} \langle \mathbf{S}_{\text{Fe}} \rangle. \quad (\text{B.3})$$

Therefore, the  $\text{Fe}^{3+}$  ions subsystem is biased by anisotropic effective exchange field of RE ions

$$\tilde{\mathbf{H}}_{\text{Re}} = \frac{2}{g\mu_B} \hat{\mathbf{A}} \langle \mathbf{S}_{\text{Re}} \rangle,$$

where  $g = 2$ . To calculate this contribution it is necessary to find the mean spin of  $\text{Eu}^{3+}$ . Using the second term of Hamiltonian (B.3) we obtain the next anisotropic exchange field from AFM  $\text{Fe}^{3+}$  sublattices in the  $i$ -direction:

$$H_{\text{exch}}^i = \frac{2J_i}{g\mu_B} \langle S_{\text{Fe}}^i \rangle, \quad (\text{B.4})$$

where

$$\begin{aligned} J_x &= J_0 \left( 1 - \frac{9}{2}G_2^0 \right) \\ J_z &= J_0 (1 + 9G_2^0). \end{aligned} \quad (\text{B.5})$$

In accordance with Wolf and Van Vleck [21], the mean spin of the RE ion induced by applied magnetic field,  $h_i$ , along the  $i$ -direction is

$$\langle S_{\text{Re}}^i \rangle = \frac{4\mu_B}{\Delta_1} (h_i + gH_{\text{exch}}^i), \quad (\text{B.6})$$

where  $\Delta_1$  is the energy level of  $\text{Eu}^{3+}$  with  $J = 1$ . Substituting (B.4) in (B.6) we obtain

$$\begin{aligned} \langle S_{\text{Re}}^i \rangle &= \frac{4\mu_B}{\Delta_1} \left( h_i + \frac{2J_i}{\mu_B} \langle S_{\text{Fe}}^i \rangle \right) \\ &= \frac{4\mu_B h_i}{\Delta_1} + \frac{8J_i}{\Delta_1} \langle S_{\text{Fe}}^i \rangle. \end{aligned} \quad (\text{B.7})$$

Therefore, the effective exchange field of  $\text{Fe}^{3+}$  ions acting on the  $\text{RE}^{3+}$  ions is presented as

$$\begin{aligned} \tilde{H}_{\text{Re}}^i &= \frac{2}{g\mu_B} J_i \left( \frac{4\mu_B h_i}{\Delta_1} + \frac{8J_i}{\Delta_1} \langle S_{\text{Fe}}^i \rangle \right) \\ &= \frac{4J_i h_i}{\Delta_1} + \frac{8J_i^2}{\mu_B \Delta_1} \langle S_{\text{Fe}}^i \rangle. \end{aligned}$$

Then the parameter  $B_{12}$  has the form

$$B_{12} = \frac{8(J_z^2 - J_x^2)}{\Delta_1}. \quad (\text{B.8})$$

As before it is supposed that the anisotropy is single axis and isotropic part of exchange  $J_{12}(0)$  now designates the sum  $J_{12}(0) + \frac{8J_x^2}{\Delta_1}$ . One can see from (B.8), at  $B_{12} < 0$  the  $J_x > J_z$  inequality for components of exchange parameter is realized.

Since the contributions of RE subsystem to  $g$ -factor of  $\text{Fe}^{3+}$  ion along the  $z$  and  $x$  axes are 0.24 and 0.22, respectively, we can find  $\Delta g_z$  and  $\Delta g_x$  analytically. It is easy to make having in mind that the magnetic field induced magnetization of the RE subsystem in accordance with (B.7) has a form

$$\langle M_{\text{Re}}^i \rangle = \frac{8\mu_B N_A h_i}{\Delta_1} + \frac{16\mu_B N_A J_i}{\Delta_1} \langle S_{\text{Fe}}^i \rangle. \quad (\text{B.9})$$

At the same time the temperature dependent contribution from  $\text{Fe}^{3+}$  sublattice can be presented as

$$\langle S_{\text{Fe}}^i \rangle = \frac{3C}{\mu_B g N_A (T - \theta_i)} h_i,$$

where  $C = \frac{1}{3k_B} S(S+1)\mu_B^2 g^2 N_A$  is the Curie constant of  $\text{Fe}^{3+}$  subsystem which will be isotropic excluding the RE contribution. The coefficient 3 is introduced because the elementary cell has three  $\text{Fe}^{3+}$  ions. Then from (B.9) we obtain the susceptibility of RE subsystem

$$\chi_{\text{Re}}^i = \frac{8\mu_B N_A}{\Delta_1} + \frac{48J_i C}{\Delta_1 g (T - \theta_i)}. \quad (\text{B.10})$$

Therefore, the correction  $\Delta C_i$  to  $C$  is equal to

$$\Delta C_i = \frac{48J_i C}{\Delta_1 g}.$$

The total Curie constant from (1) is presented as the sum. Therefore, the correction  $\Delta C_i$  to  $C$  is equal to

$$C_i = C + \Delta C_i = C \left( 1 + \frac{48J_i}{\Delta_1 g} \right),$$

that gives the value of  $g$ -factor along the  $i$  axis (for  $J_i \ll \Delta_1$ ):

$$g_i = \sqrt{\frac{3k_B C_i}{S(S+1)\mu_B^2 N_A}} \approx g \left( 1 + \frac{24J_i}{\Delta_1 g} \right).$$

Thus, the corrections to  $g$ -factor of the  $\text{Fe}^{3+}$  ions has the form

$$\Delta g_i = \frac{24J_i}{\Delta_1}. \quad (\text{B.11})$$

## References

1. G. Glasse, A. Brill, Phys. Stat. Sol. **20**, 551 (1967)
2. V.I. Chani, M.I. Timoschekhin, K. Inoue, K. Shimamura, T. Fukuda, Inorg. Mater. **30**, 1466 (1992)
3. Y. Hinatsu, Y. Doi, K. Ito, M. Wakeshima, A. Alemi, J. Solid State Chem. **172**, 438 (2003)
4. A.D. Balaev, L.N. Bezmaternykh, I.A. Gudim, V.L. Temerov, S.G. Ovchinnikov, S.A. Kharlamova, J. Magn. Mater. **258-259**, 532 (2003)
5. A.I. Pankrats, G.A. Petrakovski, L.N. Bezmaternikh, O.À. Bayukov, JETP **99**, 766 (2004)
6. A.M. Kadomtseva, A.K. Zvezdin, A.P. Piatakov, A.V. Kuvardin, Yu.F. Popov, G.P. Vorob'ev, L.N. Bezmaternykh, JETP **105**, 116 (2007)
7. F. Yen, B. Lorenz, Y.Y. Sun, C.W. Chu, L.N. Bezmaternykh, A.N. Vasiliev, Phys. Rev. B **73**, 054435 (2006)
8. N. Hur, S. Park, P.A. Sharma, J.S. Ahn, S. Guha, S.-W. Cheong, Nature **429**, 392 (2004)
9. D.I. Khomskii, J. Magn. Mater. **306**, 1 (2006)
10. A.K. Zvezdin, G.P. Vorob'ev, A.M. Kadomtseva, Yu. F. Popov, A.P. Pyatakov, L.N. Bezmaternykh, A.V. Kuvardin, E.A. Popova, JETP **83**, 509 (2006)
11. A.K. Zvezdin, S.S. Krotov, A.M. Kadomtseva, G.P. Vorob'ev, Yu.F. Popov, A.P. Pyatakov, L.N. Bezmaternykh, E.A. Popova, JETP Lett. **81**, 272 (2005)
12. A.N. Vasiliev, E.A. Popova, I.A. Gugim, L.N. Bezmaternykh, Z. Hiroi, J. Magn. Mater. **300**, e382 (2006)
13. R.Z. Levitin, E.A. Popova, R.M. Chtsherbov, A.N. Vasiliev, M.N. Popova, E.P. Chukalina, S.A. Klimin, P. van Loosdrecht, D. Fausti, L.N. Bezmaternykh, JETP Lett. **79**, 531 (2004)
14. E.A. Popova, D.V. Volkov, A.N. Vasiliev, A.A. Demidov, N.P. Kolmakova, I.A. Gugim, L.N. Bezmaternykh, N. Tristan, Yu. Skourski, B. Büchner, C. Hess, R. Klingeler, Phys. Rev. B **75**, 224413 (2007)
15. E.A. Popova, N. Tristan, A.N. Vasiliev, V.L. Temerov, L.N. Bezmaternykh, N. Leps, B. Büchner, R. Klingeler, Eur. Phys. J. B **62**, 123 (2008).
16. E.A. Popova, A.N. Vasiliev, V.L. Temerov, L.N. Bezmaternykh, N. Tristan, R. Klingeler, B. Büchner, J. Phys.: Condens. Matter **22**, 116006 (2010).
17. J.A. Campa, C. Cascales, E. Gutierrez-Puebla, M.A. Monge, I. Raines, C. Ruiz-Valero, Chem. Mater. **9**, 237 (1997)
18. D. Fausti, A. Nugroho, P. van Loosdrecht, S.A. Klimin, M.N. Popova, L.N. Bezmaternykh, Phys. Rev. B **74**, 024403 (2006)
19. L. Bezmaternykh, S. Kharlamova, V. Temerov, Krystallografiya **49**, 945 (2004)
20. A.N. Vasiliev, E.A. Popova, Low Temp. Phys. **32**, 735 (2006)
21. W.P. Wolf, J.H. Van Vleck, Phys. Rev. **118**, 1490 (1960)
22. U. Atzmony, E.R. Bauminger, A. Mustachi, I. Nowik, S. Ofer, M. Tassa, Phys. Rev. **179**, 514 (1969)
23. A. Abragam, B. Bleaney, *Electron paramagnetic resonance of transition ions* (Mir, Moskva, 1972)